Supporting Information

Multifunctional Flexible Electromagnetic Interference Shielding AgNWs/Cellulose Films with Excellent Thermal Management and Joule Heating Performances

Chaobo Liang, Kunpeng Ruan, Yali Zhang, Junwei Gu*

Shaanxi Key Laboratory of Macromolecular Science and Technology, School of Chemistry and Chemical Engineering, Northwestern Polytechnical University, Xi' an 710072, P.R. China.

Corresponding Authors: gjw@nwpu.edu.cn or nwpugjw@163.com (J. Gu)

Supplementary Figures

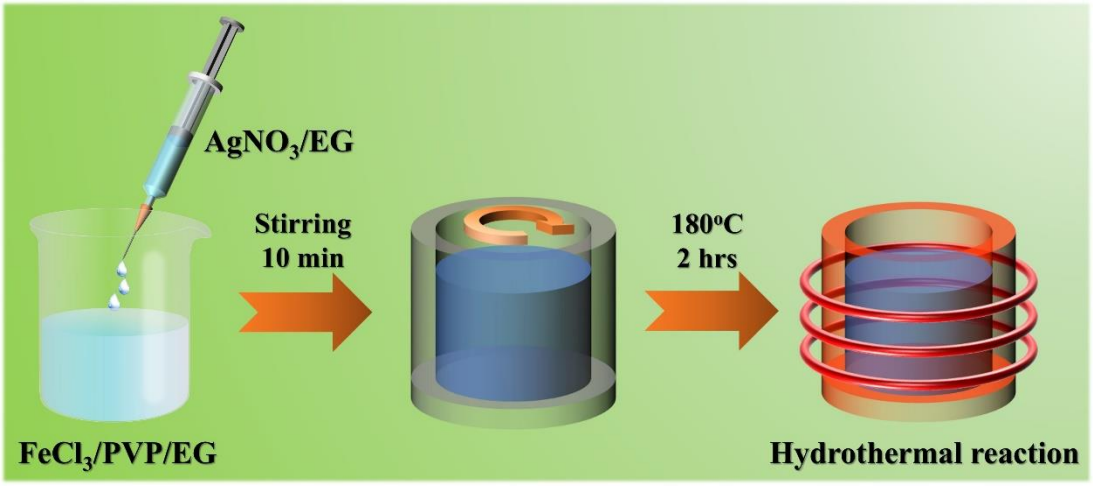

Figure S1 Schematic illustration for the fabrication process of AgNWs.

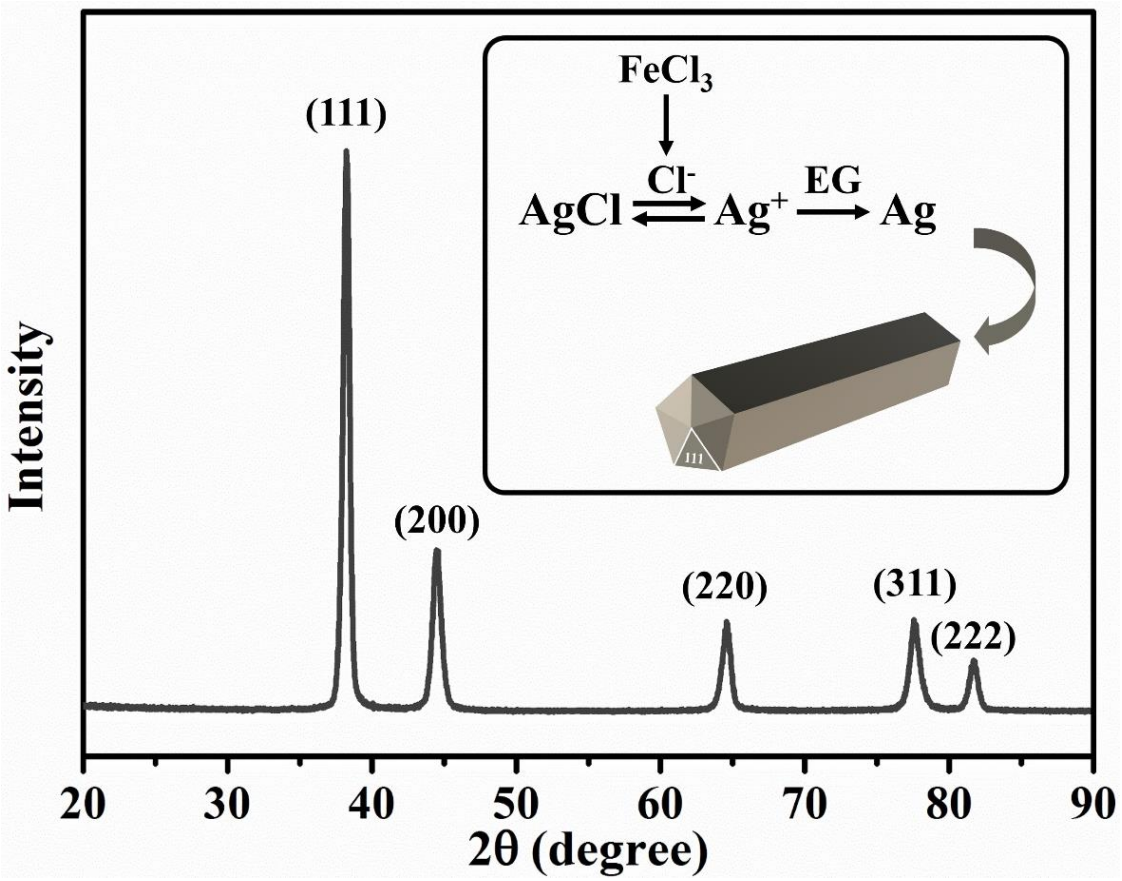

Figure S2 XRD pattern showing the growth mechanism of the AgNWs.

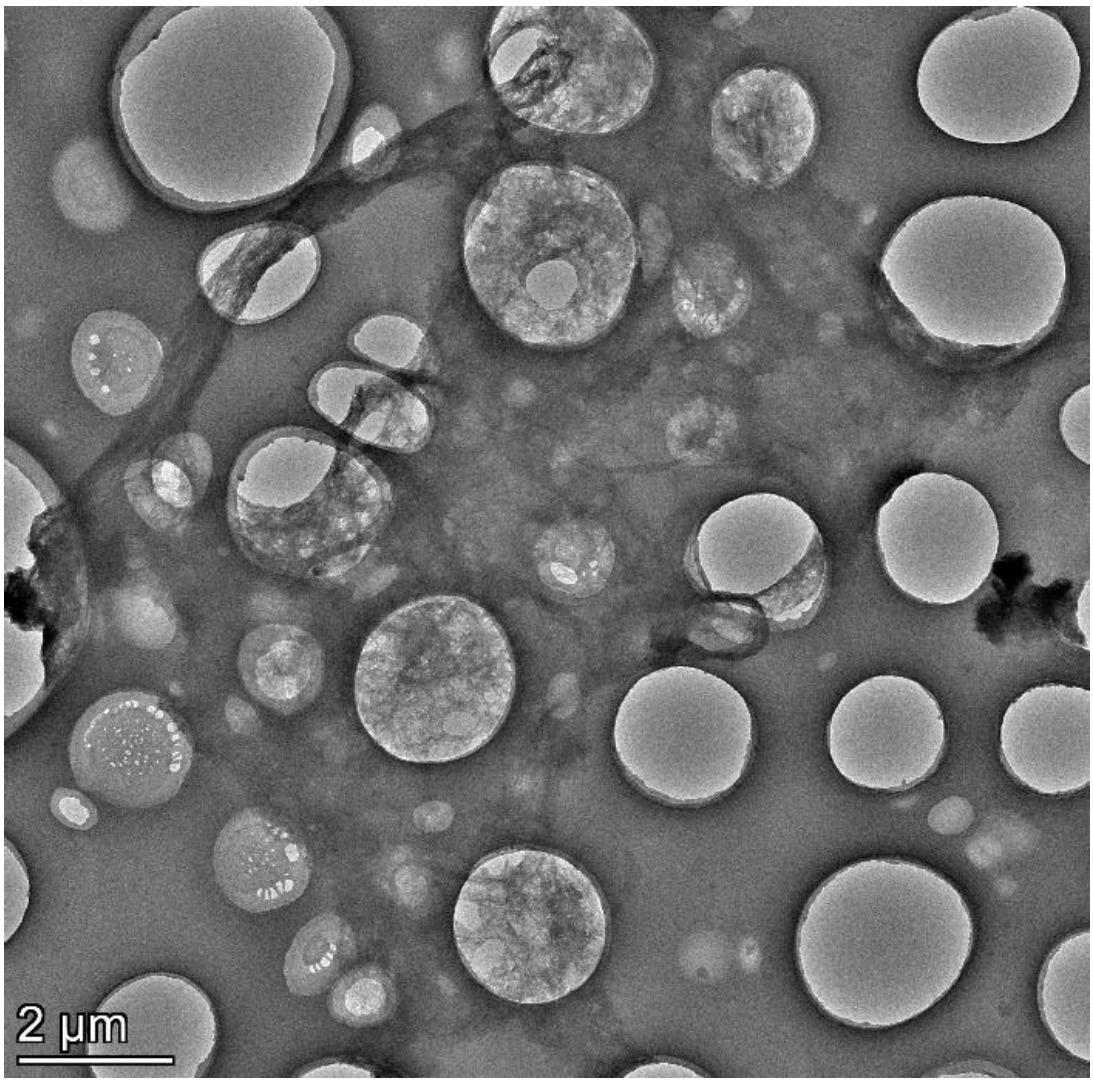

Figure S3 TEM image of cellulose.

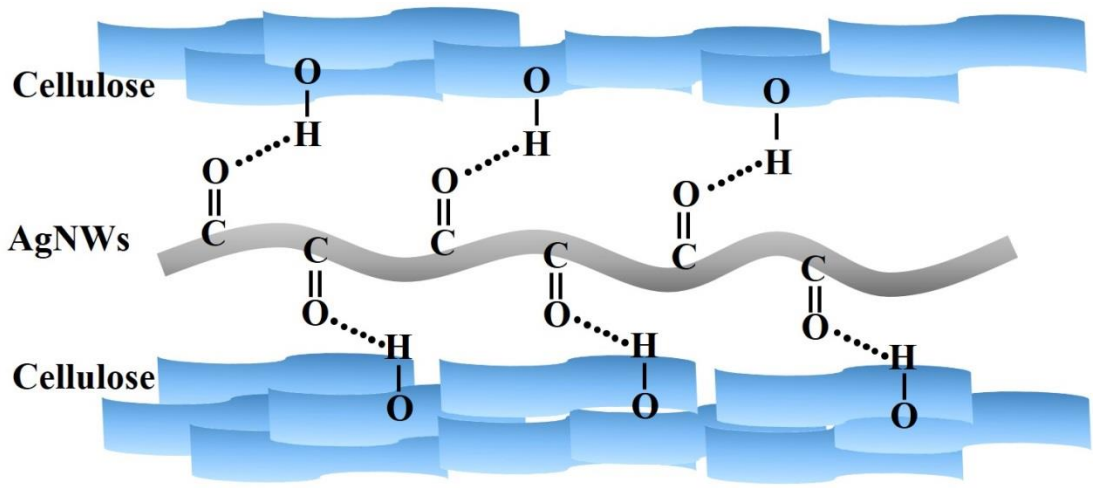

Figure S4 Schematic illustration for fabrication of the AgNWs/cellulose films.

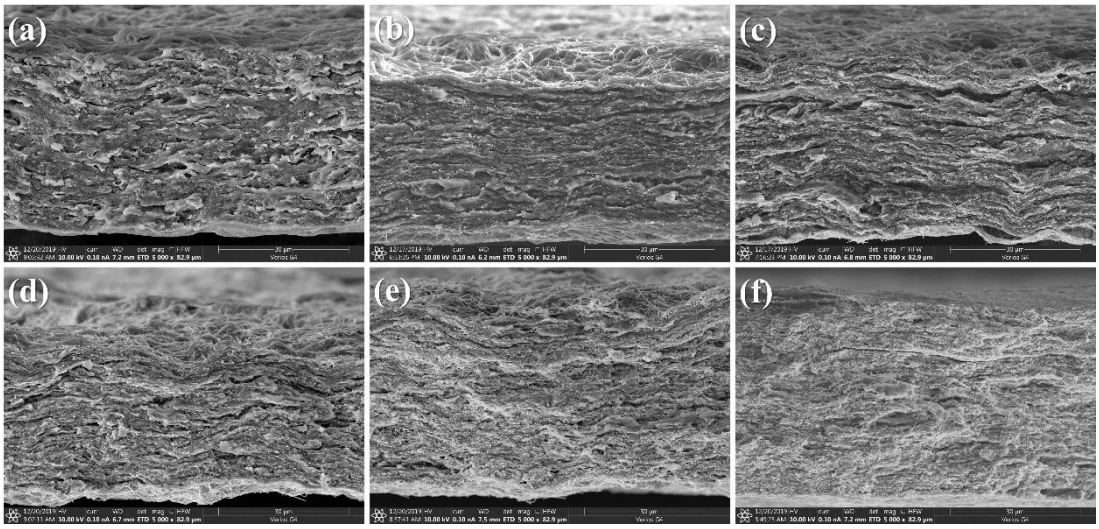

Figure S5 Cross-sectional SEM images of AgNWs/cellulose films with (a) 0, (b) 10, (c) 20, (d) 30, (e) 40 and (f) 50 wt% AgNWs.

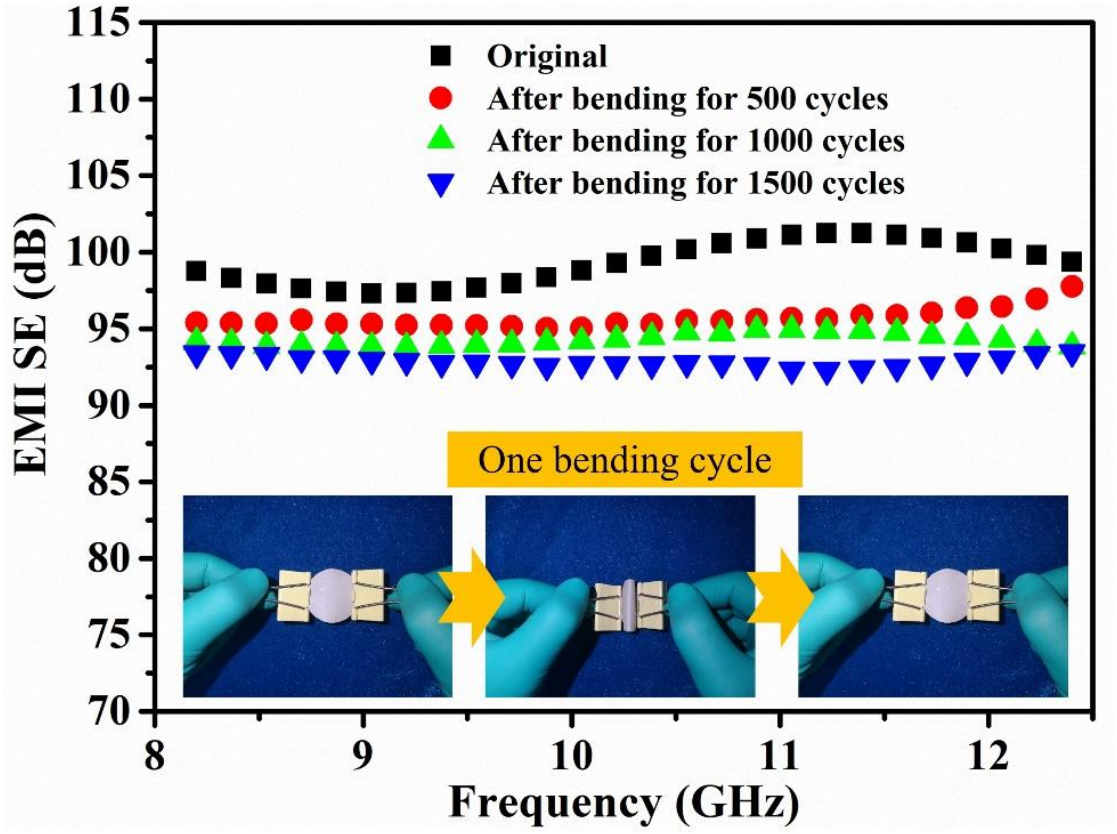

Figure S6 Variation of EMI SE of the AgNWs/cellulose films with 50 wt% AgNWs before and after bending for 1500 cycles (one bending cycle shown in the insets).

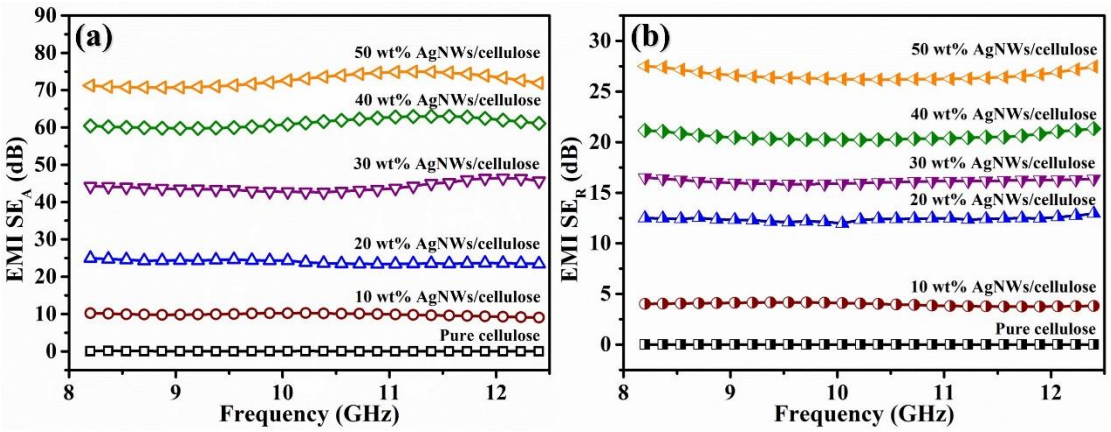

Figure S7 EMI (a) SE_A and (b) SE_R of AgNWs/cellulose films with different content of AgNWs.

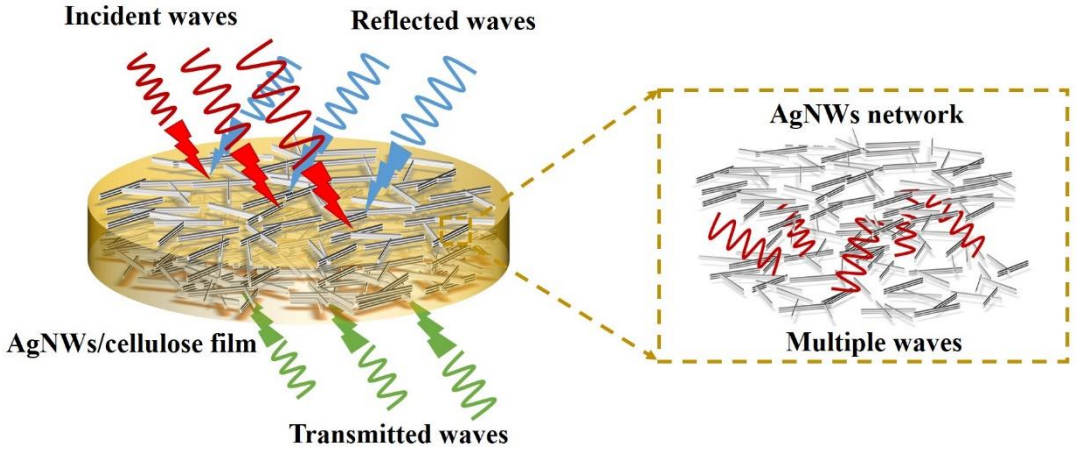

Figure S8 Schematic illustration of the electromagnetic waves transferring across the AgNWs/cellulose film.

Supplementary Note 1

Calculation of EMI shielding effectiveness (SE)

In a vector network analyzer, S_{11}, S_{12}, S_{21} and S_{22} represent reflection coefficient, transmission coefficient, back ward transmission coefficient and reverse reflection coefficient, respectively. SE_T is evaluated from the S parameters by using the following equations:

$$SE_T\left(dB\right) = -10\log\left(S_{12}^2\right) = -10\log\left(S_{21}^2\right) = -10\log\left(T\right) \quad (1)$$

$$SE_R\left(dB\right) = -10\log\left(1-S_{11}^2\right) = -10\log\left(1-R\right) \quad (2)$$

$$SE_A\left(dB\right) = -10\log\left(\frac{S_{12}^2}{1-S_{11}^2}\right) = -10\log\left(\frac{T}{1-R}\right) \quad (3)$$

Supplementary Methods

Materials: Cotton was purchased from Jinzhong Sanitary Materials Co., Ltd. Urea (99%), ferric chloride hydrate ($FeCl_3$ $6H_2O$, 99%), poly vinylpyrrolidone (PVP, M_w = 58,000), ethylene glycol (EG, ≥99.0%), ethanol (95%) were all supplied by Aladdin Reagent Co., Ltd, China. Sodium hydroxide (NaOH, analytical grade) and acetone (analytical grade) were both purchased from Beijing Chemical Factory, China. Silver nitrate ($AgNO_3$, ≥99.999%) was received from Sigma-Aldrich Co. Ltd., USA.

Characterizations: X-ray photoelectron spectroscopy (XPS) analyses of the samples were carried out using PHI5400 equipment (PE Corp., England). X-ray diffraction (XRD) crystallography of the samples was obtained on a Phillips PW3040-MPD diffractometer (Royal Philips Corp., Netherlands). Scanning electron microscopy (SEM) images of the samples were analyzed by Verios G4 equipment (FEI Corp., America). Transmission electron microscope (TEM) morphologies of the samples were analyzed by FEI Talos F200X TEM (FEI Corp., America). Thermal conductivity coefficient (λ) and thermal diffusivity (α) values of the samples were measured using a TPS2200 Hot Disk instrument (AB Corp., Sweden) by the transient plane source method according to standard ISO 22007-2:2008. Thermal images of the samples were taken by a infrared thermal imager of Ti 300 equipment (Fluke Corp., America). Electrical conductivities of the samples were collected by RTS-8 (Guangzhou Four Probes Technology Corp., China). Characteristic EMI shielding parameters of the samples were tested by MS4644A Vector Network Analyzer instrument (Anritsu Corp., Japan) using the wave-guide method at X-band according to ASTM D5568-08. Tensile strength of the samples was tested by Instron electronic tensile machine according to standard ASTM D412, and the sample size was 230 mm × 15 mm.

Supplementary Table

Table S1 Comparison of EMI shielding performances for different materials

Type	Materials	Thickness (mm)	σ (S/m)	EMI SE (dB)	Ref
Reduced graphene oxide (rGO)	rGO/PS	2.5	43.5	45.1	1
	rGO/PEI	2.3	0.001	22	2
	rGO/PDMS	1	180	30	3
	rGO/Wax	2	/	29	4
	rGO/Wax	0.35	2500	27	5
	rGO/WPU	1	16.8	34	6
	rGO/EP	/	10	21	7
	rGO/PS	2.5	1.25	29	8
	rGO/PU	60	0.06	39.4	9
	rGO/PI	0.073	2×10^{5}	51	10
	rGO/PANI	2.8	1800	34.2	11
	S-doped rGO/PS	2	33	24.5	12
rGO with Fe_2O_3 or Fe_3O_4	rGO/Fe_2O_3/PVA	0.36	3	20.3	5
	rGO/Fe_2O_3/PANI	2.5	80	51	13
	rGO/Fe_3O_4/PVA	0.3	/	15	14
	rGO/Fe_3O_4/PANI	2.5	260	30	15
	rGO/CF/Fe_2O_3	0.4	1.7×10^{4}	41.8	16
	rGO/Fe_3O_4/PVC	1.8	7.7×10^{-4}	13	17
	rGO/Fe_3O_4/PEI	2.5	10^{-4}	18	18
graphite	graphite/PA66	3.2	/	12	19
	graphite/PE	2.5	10	51.6	20
	graphite/PE	3	/	33	21
	graphite/EP	5	2.6	11	22
	graphite/ABS	3	16	60	23
Carbon nanotubes (CNTs)	MWCNTs/WPU	0.8	2.1×10^{3}	80	24
	CNTs/EP	2	516	33	25
	MWCNTs/WPU	4.5	44.6	50	10
	MWCNTs/Cellulose	0.15	/	35	26
	MWCNTs/PMMA	0.165	1000	27	27
	MWCNTs/PEDOT	2.8	1935	58	28
	MWCNTs/PTT	2	30	42	29

	SWCNTs/EP	2	20	25	30
	SWCNTs/PU	2	2.2×10^{-4}	17	31
	CNTs/PS	/	/	18.5	32
	CNTs/Coal tar	0.6	1.1×10^{3}	56	33
Carbon fiber (CF)	CF/Fe_3O_4/EP	13	0.2	20	34
	CF/Fe_3O_4/PDMS	0.7	710	67.9	35
	CF/PES	2.87	/	38	36
	CF/PVDF	0.05	180	14	37
	CF/PP	3.2	10	25	38
	CF/PS	/	0.1	19	39
	CF/CNT/PS	1	0.215	21.9	40
	CF/GN/Was	0.27	800	28	41
Metals	Ni	3	100	20	42
	Ni/CB	1	31.6	85	43
	Ni	1.95	/	23	44
	Ni fiber	2.85	/	58	45
	Ni-co fiber	2.5	1.3×10^{3}	41.2	46
	Ag/CF	2.5	/	38	47
	Cu/graphite	2	80	70	48
	CuNWs	0.2	/	35	49
	Al	2.9	/	39	36
	SS	3.1	0.1	48	50
	Mxene/SA	0.008	2.9×10^{5}	57	51
	AgNWs/cellulose	***0.0445***	***5.57×10^{5}***	***101***	***This work***

***PS, PEDOT, ABS, CB, SS, PES, PEI, PMMA, PDMS, PP, PI, WPU, EP, PU, PANI, PVA, PVC, PE, PA66, PVDF, PTT, CuNWs and SA represents polystyrene, poly(3,4-ethylenedioxythiophene), acrylonitrile-butadiene-styrene, carbon black, stainless steel, polyethersulfone, polyetherimide, polymethylmethacrylate, poly(dimethyl siloxane), polypropylene, polyimide, waterborne polyurethane, epoxy, polyurethane, polyaniline, polyvinyl alcohol, polyvinyl chloride, polyethylene, nylon 66, Poly(vinylidene fluoride), polytrimethylene-tereph-thalate, copper nanowires and sodium alginate, respectively.

Table S2 Comparison of EMI SE and λ for different materials

Type	Materials	Thickness (mm)	EMI SE (dB)	λ W/mK	Ref
Carbon fillers	rGO-WPU/cotton	1	46	2.13	52
	SEBS-g-MAH/f-BN	4	38	12.6	53
	RGO@Fe3O4/epoxy	1	13	1.2	54
	GNPs/PS	3	33	4.72	55
	GNPs/rGO/epoxy	3	51	1.56	56
	RGO/CNF	0.023	26	7.3	57
	GNP/PEDOT:PSS	0.8	70	0.83	58
Carbon-metal hybrid fillers	APCF-epoxy	2.5	38	2.49	47
	GNSs/CINAP/CE	3.5	55	4.13	59
	PVDF/CNT/Ni	0.6	57	0.65	60
	PVDF/GNP/Ni	0.6	56	0.66	60
	PVDF/CNT/Co-chain	0.3	35	1.39	61
	PVDF/CNT/Co-flower	0.3	32	1.3	61
	MWCNT-Fe_3O_4@Ag/epoxy	2	35	0.46	62
	PVDF/Fe_3O_4/CNT	1.1	33	0.62	63
	PVDF/Fe_3O_4/GNP	1.1	36	0.68	63
Metal fillers	PVA/MXene	0.027	44	4.6	64
	PVA/MXene	0.025	37	3.3	64
	PCL/Cu hollow bead	1	110	7	65
	CuNWs-TAGA/epoxy	3	47	0.51	66
	epoxy/$SnBi_{58}$	2	72	1.6	67
	AgNWs/cellulose	***0.0445***	***101***	***10.55***	***This work***

***PVA, CuNWs, rGO, WPU, SEBS-g-MAH, BN, GNPs, PS, CNF, APCF, CINAP, PEDOT:PSS, CE, PVDF, CNT represents poly(vinyl alcohol), copper nanowires, reduced graphene oxide, waterborne polyurethane, styrene-ethylene/butylene-styrene, boron nitride, graphene nanoplatelets, polystyrene, cellulose nanofiber, Ag-plating carbon fiber, magnetic carbonyl iron-nickel alloy, poly(3,4-ethylenedioxythiophene)-poly(styrenesulfonate), cyanate ester, poly(vinylidene fluoride), carbon nanotube, respectively.

Supplementary References

(1) Yan, D.-X.; Pang, H.; Li, B.; Vajtai, R.; Xu, L.; Ren, P.-G.; Wang, J.-H.; Li, Z.-M. Structured reduced graphene oxide/polymer composites for ultra-efficient electromagnetic interference shielding. *Adv. Funct. Mater.* **2015,** *25*, 559-566.

(2) Ling, J.; Zhai, W.; Feng, W.; Shen, B.; Zhang, J.; Zheng, W. G. Facile preparation of lightweight microcellular polyetherimide/graphene composite foams for electromagnetic interference shielding. *ACS Appl. Mater. Interfaces* **2013,** *5*, 2677-2684.

(3) Chen, Z.; Xu, C.; Ma, C.; Ren, W.; Cheng, H.-M. Lightweight and flexible graphene foam composites for high-performance electromagnetic interference shielding. *Adv. Mater.* **2013,** *25*, 1296-1300.

(4) Wen, B.; Wang, X. X.; Cao, W. Q.; Shi, H. L.; Lu, M. M.; Wang, G.; Jin, H. B.; Wang, W. Z.; Yuan, J.; Cao, M. S. Reduced graphene oxides: the thinnest and most lightweight materials with highly efficient microwave attenuation performances of the carbon world. *Nanoscale* **2014,** *6*, 5754-5761.

(5) Yuan, B.; Bao, C.; Qian, X.; Song, L.; Tai, Q.; Liew, K. M.; Hu, Y. Design of artificial nacre-like hybrid films as shielding to mitigate electromagnetic pollution. *Carbon* **2014,** *75*, 178-189.

(6) Hsiao, S.-T.; Ma, C.-C. M.; Liao, W.-H.; Wang, Y.-S.; Li, S.-M.; Huang, Y.-C.; Yang, R.-B.; Liang, W.-F. Lightweight and flexible reduced graphene oxide/water-borne polyurethane composites with high electrical conductivity and excellent electromagnetic interference shielding performance. *ACS Appl. Mater.*

Interfaces **2014,** *6*, 10667-10678.

(7) Liang, J.; Wang, Y.; Huang, Y.; Ma, Y.; Liu, Z.; Cai, J.; Zhang, C.; Gao, H.; Chen, Y. Electromagnetic interference shielding of graphene/epoxy composites. *Carbon* **2009,** *47*, 922-925.

(8) Yan, D.-X.; Ren, P.-G.; Pang, H.; Fu, Q.; Yang, M.-B.; Li, Z.-M. Efficient electromagnetic interference shielding of lightweight graphene/polystyrene composite. *J. Mater. Chem.* **2012,** *22*, 18772-18774.

(9) Shen, B.; Li, Y.; Zhai, W.; Zheng, W. Compressible graphene-coated polymer foams with ultralow density for adjustable electromagnetic interference (EMI) shielding. *ACS Appl. Mater. Interfaces* **2016,** *8*, 8050-8057.

(10) Zeng, Z.; Jin, H.; Chen, M.; Li, W.; Zhou, L.; Zhang, Z. Lightweight and anisotropic porous MWCNT/WPU composites for ultrahigh performance electromagnetic interference shielding. *Adv. Funct. Mater.* **2016,** *26*, 303-310.

(11) Yuan, B.; Yu, L.; Sheng, L.; An, K.; Zhao, X. Comparison of electromagnetic interference shielding properties between single-wall carbon nanotube and graphene sheet/polyaniline composites. *J. Appl. Phys.* **2012,** *45*, 235108.

(12) Shahzad, F.; Yu, S.; Kumar, P.; Lee, J.-W.; Kim, Y.-H.; Hong, S. M.; Koo, C. M. Sulfur doped graphene/polystyrene nanocomposites for electromagnetic interference shielding. *Compos. Struct.* **2015,** *133*, 1267-1275.

(13) Singh, A. P.; Mishra, M.; Sambyal, P.; Gupta, B. K.; Singh, B. P.; Chandra, A.; Dhawan, S. K. Encapsulation of gamma-Fe_2O_3 decorated reduced graphene oxide in polyaniline core-shell tubes as an exceptional tracker for electromagnetic

environmental pollution. *J. Mater. Chem. A* **2014,** *2*, 3581-3593.

(14) Rao, B. V. B.; Yadav, P.; Aepuru, R.; Panda, H. S.; Ogale, S.; Kale, S. N. Single-layer graphene-assembled 3D porous carbon composites with PVA and Fe_3O_4 nano-fillers: an interface-mediated superior dielectric and EMI shielding performance. *PCCP* **2015,** *17*, 18353-18363.

(15) Singh, K.; Ohlan, A.; Viet Hung, P.; Balasubramaniyan, R.; Varshney, S.; Jang, J.; Hur, S. H.; Choi, W. M.; Kumar, M.; Dhawan, S. K.; Kong, B.-S.; Chung, J. S. Nanostructured graphene/Fe_3O_4 incorporated polyaniline as a high performance shield against electromagnetic pollution. *Nanoscale* **2013,** *5*, 2411-2420.

(16) Singh, A. P.; Garg, P.; Alam, F.; Singh, K.; Mathur, R. B.; Tandon, R. P.; Chandra, A.; Dhawan, S. K. Phenolic resin-based composite sheets filled with mixtures of reduced graphene oxide, gamma-Fe_2O_3 and carbon fibers for excellent electromagnetic interference shielding in the X-band. *Carbon* **2012,** *50*, 3868-3875.

(17) Yao, K.; Gong, J.; Tian, N.; Lin, Y.; Wen, X.; Jiang, Z.; Na, H.; Tang, T. Flammability properties and electromagnetic interference shielding of PVC/graphene composites containing Fe_3O_4 nanoparticles. *RSC Adv.* **2015,** *5*, 31910-31919.

(18) Shen, B.; Zhai, W.; Tao, M.; Ling, J.; Zheng, W. Lightweight, multifunctional polyetherimide/graphene@Fe_3O_4 composite foams for shielding of electromagnetic pollution. *ACS Appl. Mater. Interfaces* **2013,** *5*, 11383-11391.

(19) Krueger, Q. J.; King, J. A. Synergistic effects of carbon fillers on shielding effectiveness in conductive nylon 6,6-and polycarbonate-based resins. *Adv. Polym. Tech.* **2003,** *22*, 96-111.

(20) Jiang, X.; Yan, D.-X.; Bao, Y.; Pang, H.; Ji, X.; Li, Z.-M. Facile, green and affordable strategy for structuring natural graphite/polymer composite with efficient electromagnetic interference shielding. *RSC Adv.* **2015,** *5* (29), 22587-22592.

(21) Panwar, V.; Mehra, R. M. Analysis of electrical, dielectric, and electromagnetic interference shielding behavior of graphite filled high density polyethylene composites. *Polym. Eng. Sci.* **2008,** *48*, 2178-2187.

(22) De Bellis, G.; Tamburrano, A.; Dinescu, A.; Santarelli, M. L.; Sarto, M. S. Electromagnetic properties of composites containing graphite nanoplatelets at radio frequency. *Carbon* **2011,** *49*, 4291-4300.

(23) Sachdev, V. K.; Patel, K.; Bhattacharya, S.; Tandon, R. P. Electromagnetic interference shielding of graphite/acrylonitrile butadiene styrene composites. *J. Appl. Polym. Sci.* **2011,** *120*, 1100-1105.

(24) Zeng, Z.; Chen, M.; Jin, H.; Li, W.; Xue, X.; Zhou, L.; Pei, Y.; Zhang, H.; Zhang, Z. Thin and flexible multi-walled carbon nanotube/waterborne polyurethane composites with high-performance electromagnetic interference shielding. *Carbon* **2016,** *96*, 768-777.

(25) Chen, Y.; Zhang, H.-B.; Yang, Y.; Wang, M.; Cao, A.; Yu, Z.-Z. High-performance epoxy nanocomposites reinforced with three-dimensional carbon nanotube sponge for electromagnetic interference shielding. *Adv. Funct. Mater.* **2016,** *26* (3), 447-455.

(26) Wang, L.-L.; Tay, B.-K.; See, K.-Y.; Sun, Z.; Tan, L.-K.; Lua, D. Electromagnetic interference shielding effectiveness of carbon-based materials prepared by screen

printing. *Carbon* **2009,** *47*, 1905-1910.

(27) Kim, H. M.; Kim, K.; Lee, C. Y.; Joo, J.; Cho, S. J.; Yoon, H. S.; Pejakovic, D. A.; Yoo, J. W.; Epstein, A. J. Electrical conductivity and electromagnetic interference shielding of multiwalled carbon nanotube composites containing Fe catalyst. *Appl. Phys. Lett.* **2004,** *84*, 589-591.

(28) Farukh, M.; Singh, A. P.; Dhawan, S. K. Enhanced electromagnetic shielding behavior of multi-walled carbon nanotube entrenched poly (3,4-ethylenedioxythiophene) nanocomposites. *Compos. Sci. Technol.* **2015,** *114*, 94-102.

(29) Gupta, A.; Choudhary, V. Electromagnetic interference shielding behavior of poly(trimethylene terephthalate)/multi-walled carbon nanotube composites. *Compos. Sci. Technol.* **2011,** *71*, 1563-1568.

(30) Huang, Y.; Li, N.; Ma, Y.; Feng, D.; Li, F.; He, X.; Lin, X.; Gao, H.; Chen, Y. The influence of single-walled carbon nanotube structure on the electromagnetic interference shielding efficiency of its epoxy composites. *Carbon* **2007,** *45*, 1614-1621.

(31) Liu, Z.; Bai, G.; Huang, Y.; Ma, Y.; Du, F.; Li, F.; Guo, T.; Chen, Y. Reflection and absorption contributions to the electromagnetic interference shielding of single-walled carbon nanotube/polyurethane composites. *Carbon* **2007,** *45*, 821-827.

(32) Yang, Y. L.; Gupta, M. C. Novel carbon nanotube-polystyrene foam composites for electromagnetic interference shielding. *Nano Lett.* **2005,** *5*, 2131-2134.

(33) Chaudhary, A.; Kumari, S.; Kumar, R.; Teotia, S.; Singh, B. P.; Singh, A. P.;

Dhawan, S. K.; Dhakate, S. R. Lightweight and easily foldable MCMB-MWCNTs composite paper with exceptional electromagnetic interference shielding. *ACS Appl. Mater. Interfaces* **2016,** *8*, 10600-10608.

(34) Crespo, M.; Mendez, N.; Gonzalez, M.; Baselga, J.; Pozuelo, J. Synergistic effect of magnetite nanoparticles and carbon nanofibres in electromagnetic absorbing composites. *Carbon* **2014,** *74*, 63-72.

(35) Bayat, M.; Yang, H.; Ko, F. K.; Michelson, D.; Mei, A. Electromagnetic interference shielding effectiveness of hybrid multifunctional Fe_3O_4/carbon nanofiber composite. *Polymer* **2014,** *55*, 936-943.

(36) Li, L.; Chung, D. D. L. Electrical and mechanical-properties of electrically conductive polyethersulfone composites. *Composites* **1994,** *25*, 215-224.

(37) Lee, B. O.; Woo, W. J.; Park, H. S.; Hahm, H. S.; Wu, J. P.; Kim, M. S. Influence of aspect ratio and skin effect on EMI shielding of coating materials fabricated with carbon nanofiber/PVDF. *J. Mater. Sci.* **2002,** *37*, 1839-1843.

(38) Ameli, A.; Jung, P. U.; Park, C. B. Electrical properties and electromagnetic interference shielding effectiveness of polypropylene/carbon fiber composite foams. *Carbon* **2013,** *60*, 379-391.

(39) Yang, Y. L.; Gupta, M. C.; Dudley, K. L.; Lawrence, R. W. Conductive carbon nanoriber-polymer foam structures. *Adv. Mater.* **2005,** *17*, 1999-2003.

(40) Yang, Y.; Gupta, M. C.; Dudley, K. L. Towards cost-efficient EMI shielding materials using carbon nanostructure-based nanocomposites. *Nanotechnology* **2007,** *18*, 345701.

(41) Song, W.-L.; Wang, J.; Fan, L.-Z.; Li, Y.; Wang, C.-Y.; Cao, M.-S. Interfacial engineering of carbon nanofiber-graphene-carbon nanofiber heterojunctions in flexible lightweight electromagnetic shielding networks. *ACS Appl. Mater. Interfaces* **2014,** *6*, 10516-10523.

(42) Wenderoth, K.; Petermann, J.; Kruse, K. D.; Terhaseborg, J. L.; Krieger, W. Synergism on electromagnetic inductance (EMI)-shielding in metal-particle and ferroelectric-particle filled polymers. *Polym. Compos.* **1989,** *10*, 52-56.

(43) El-Tantawy, F.; Aal, N. A.; Sung, Y. K. New functional conductive polymer composites containing nickel coated carbon black reinforced phenolic resin. *Macromol. Res.* **2005,** *13*, 194-205.

(44) Gargama, H.; Thakur, A. K.; Chaturvedi, S. K. Polyvinylidene fluoride/nickel composite materials for charge storing, electromagnetic interference absorption, and shielding applications. *J. Appl. Phys.* **2015,** *117*, 345701.

(45) Shui, X. P.; Chung, D. D. L. Nickel filament polymer-matrix composites with low surface impedance and high electromagnetic interference shielding effectiveness. *J. Electron. Mater.* **1997,** *26*, 928-934.

(46) Huang, X.; Dai, B.; Ren, Y.; Xu, J.; Zhu, P. Preparation and study of electromagnetic interference shielding materials comprised of Ni-Co coated on web-like biocarbon nanofibers via electroless deposition. *J. Nanomater.* **2015,** *2015*, 320306.

(47) Li, J.; Qi, S.; Zhang, M.; Wang, Z. Thermal conductivity and electromagnetic shielding effectiveness of composites based on Ag-plating carbon fiber and epoxy. *J.*

Appl. Polym. Sci. **2015,** *132*, 42306.

(48) Al-Ghamdi, A. A.; El-Tantawy, F. New electromagnetic wave shielding effectiveness at microwave frequency of polyvinyl chloride reinforced graphite/copper nanoparticles. *Compos. Part A-Appl. S.* **2010,** *41*, 1693-1701.

(49) Al-Saleh, M. H.; Gelves, G. A.; Sundararaj, U. Copper nanowire/polystyrene nanocomposites: lower percolation threshold and higher EMI shielding. *Compos. Part A-Appl. S.* **2011,** *42* (1), 92-97.

(50) Ameli, A.; Nofar, M.; Wang, S.; Park, C. B. Lightweight polypropylene/stainless-steel fiber composite foams with low percolation for efficient electromagnetic interference shielding. *ACS Appl. Mater. Interfaces* **2014,** *6*, 11091-11100.

(51) Shahzad, F.; Alhabeb, M.; Hatter, C. B.; Anasori, B.; Man, H. S.; Koo, C. M.; Gogotsi, Y. Electromagnetic interference shielding with 2D transition metal carbides (MXenes). *Science* **2016,** *353*, 1137-1140.

(52) Wang, Y.; Wang, W.; Xu, R.; Zhu, M.; Yu, D. Flexible, durable and thermal conducting thiol-modified rGO-WPU/cotton fabric for robust electromagnetic interference shielding. *Chem. Eng. J.* **2019,** *360*, 817-828.

(53) Zhang, X.; Zhang, X.; Yang, M.; Yang, S.; Wu, H.; Guo, S.; Wang, Y. Ordered multilayer film of (graphene oxide/polymer and boron nitride/polymer) nanocomposites: An ideal EMI shielding material with excellent electrical insulation and high thermal conductivity. *Compos. Sci. Technol.* **2016,** *136*, 104-110.

(54) Liu, Y.; Lu, M.; Wu, K.; Yao, S.; Du, X.; Chen, G.; Zhang, Q.; Liang, L.; Lu, M.

Anisotropic thermal conductivity and electromagnetic interference shielding of epoxy nanocomposites based on magnetic driving reduced graphene oxide@Fe_3O_4. *Compos. Sci. Technol.* **2019,** *174*, 1-10.

(55) Guo, Y.; Pan, L.; Yang, X.; Ruan, K.; Han, Y.; Kong, J.; Gu, J. Simultaneous improvement of thermal conductivities and electromagnetic interference shielding performances in polystyrene composites via constructing interconnection oriented networks based on electrospinning technology. *Compos. Part A-Appl. S.* **2019,** *124*, 105484.

(56) Liang, C.; Qiu, H.; Han, Y.; Gu, H.; Song, P.; Wang, L.; Kong, J.; Cao, D.; Gu, J. Superior electromagnetic interference shielding 3D graphene nanoplatelets/reduced graphene oxide foam/epoxy nanocomposites with high thermal conductivity. *J. Mater. Chem. C* **2019,** *7*, 2725-2733.

(57) Yang, W.; Zhao, Z.; Wu, K.; Huang, R.; Liu, T.; Jiang, H.; Chen, F.; Fu, Q. Ultrathin flexible reduced graphene oxide/cellulose nanofiber composite films with strongly anisotropic thermal conductivity and efficient electromagnetic interference shielding. *J. Mater. Chem. C* **2017,** *5*, 3748-3756.

(58) Agnihotri, N.; Chakrabarti, K.; De, A. Highly efficient electromagnetic interference shielding using graphite nanoplatelet/poly(3,4-ethylenedioxythiophene)-poly(styrenesulfonate) composites with enhanced thermal conductivity. *RSC Adv.* **2015,** *5*, 43765-43771.

(59) Ren, F.; Song, D.; Li, Z.; Jia, L.; Zhao, Y.; Yan, D.; Ren, P. Synergistic effect of graphene nanosheets and carbonyl iron-nickel alloy hybrid filler on electromagnetic

interference shielding and thermal conductivity of cyanate ester composites. *J. Mater. Chem. C* **2018,** *6*, 1476-1486.

(60) Zhao, B.; Wang, S.; Zhao, C.; Li, R.; Hamidinejad, M.; Kazemi, Y.; Park, C. B. Synergism between carbon materials and Ni chains in flexible poly(vinylidene fluoride) composite films with high heat dissipation to improve electromagnetic shielding properties. *Carbon* **2018,** *127*, 469-478.

(61) Li, X.; Zeng, S.; E, S.; Liang, L.; Bai, Z.; Zhou, Y.; Zhao, B.; Zhang, R. Quick heat dissipation in absorption-dominated microwave shielding properties of flexible poly(vinylidene fluoride)/carbon nanotube/Co composite films with anisotropy-shaped Co (flowers or chains). *ACS Appl. Mater. Interfaces* **2018,** *10*, 40789-40799.

(62) Wang, L.; Qiu, H.; Liang, C.; Song, P.; Han, Y.; Han, Y.; Gu, J.; Kong, J.; Pan, D.; Guo, Z. Electromagnetic interference shielding MWCNT-Fe_3O_4@Ag/epoxy nanocomposites with satisfactory thermal conductivity and high thermal stability. *Carbon* **2019,** *141*, 506-514.

(63) Cheng, H.; Wei, S.; Ji, Y.; Zhai, J.; Zhang, X.; Chen, J.; Shen, C. Synergetic effect effect of Fe_3O_4 nanoparticles and carbon on flexible poly (vinylidence fluoride) based films with higher heat dissipation to improve electromagnetic shielding. *Compos. Part A-Appl. S.* **2019,** *121*, 139-148.

(64) Jin, X.; Wang, J.; Dai, L.; Liu, X.; Li, L.; Yang, Y.; Cao, Y.; Wang, W.; Wu, H.; Guo, S. Flame-retardant poly(vinyl alcohol)/MXene multilayered films with outstanding electromagnetic interference shielding and thermal conductive

performances. *Chem. Eng. J.* **2020,** *380,* 122475.

(65) Lee, S. H.; Yu, S.; Shahzad, F.; Kim, W. N.; Park, C.; Hong, S. M.; Koo, C. M. Density-tunable lightweight polymer composites with dual-functional ability of efficient EMI shielding and heat dissipation. *Nanoscale* **2017,** *9,* 13432-13440.

(66) Yang, X.; Fan, S.; Li, Y.; Guo, Y.; Li, Y.; Ruan, K.; Zhang, S.; Zhang, J.; Kong, J.; Gu, J. Synchronously improved electromagnetic interference shielding and thermal conductivity for epoxy nanocomposites by constructing 3D copper nanowires/thermally annealed graphene aerogel framework. *Compos. Part A-Appl. S.* **2020,** *128,* 105670.

(67) Shu, M.; Zhang, P.; Ding, X.; Gong, Y.; Wang, Y.; Wang, R.; Zheng, K.; Tian, X.; Zhang, X. Low melting point alloy segregated network construction in thermosetting polymer matrix for the electromagnetic interference shielding and thermal conductivity enhancement. *Mater. Res. Express* **2019,** *6*, 115352.